# $x$-dependent polarized parton distributions

Lionel E. Gordon
*Thomas Jefferson National Lab, Newport News, Virginia 23606;*
*Hampton University, Hampton, Virginia 23668;*
*and Argonne National Lab, Argonne, Illinois 60439*

Mehrdad Goshtasbpour
*Shahid Beheshti University, Tehran, Iran*
*and Center For Theoretical Physics and Mathematics, AEOI, Tehran, Iran*

Gordon P. Ramsey
*Loyola University, Chicago, Illinois 60626*
*and Argonne National Lab, Argonne, Illinois 60439*
(Received 20 March 1998; published 28 September 1998)

Using QCD motivated and phenomenological considerations, we construct $x$ dependent polarized parton distributions, which evolve under GLAP evolution, satisfy DIS data and are within positivity constraints. Each flavor is done separately and the overall set can be used to predict polarization asymmetries for various processes. We perform our NLO analysis strictly in $x$ space. Small-$x$ results and other physical considerations are discussed. [S0556-2821(98)05819-6]

PACS number(s): 13.88.+e, 13.60.Hb, 14.20.Dh

## I. INTRODUCTION

In light of recent polarized deep-inelastic-scattering data, there has been considerable interest in generating $x$-dependent parton distributions for the spin-dependent case. Physics results have been extracted from the integrated structure functions [1–3]. The results indicate that there is still considerable uncertainty in the fraction of spin carried by the gluons and sea quarks. Each of the analyses rely on certain assumptions to model the polarized distributions. One important way to test these assumptions is to generate the $x$-dependent distributions and predict spin observables, such as the structure functions, $g_1$, for the proton, neutron and deuteron, hard scattering cross sections for polarized hadronic collisions and hadronic production of pions, kaons and heavy quark flavors. The structure function measurements of $g_1$ have been made, but the distributions at small-$x$ are still quite uncertain.

There are various sets of $x$-dependent polarized distributions which extract the unknown parameters from assumptions about the data [3–9]. Most of these are consistent with the $x$-dependent data, but do not adequately address the physical questions of compatibility with the integrated data (and hence the spin fractions of the partons) and the positivity constraints for each flavor. The usual approach is to fit the polarized data directly with a given parametrization, and then check the integrals for agreement with the extracted fractions of spin carried by the quark flavors (or set normalizations to fit the spin fractions). Often, either the valence is not considered separately or the flavor dependence of the sea is not considered.

Our approach is to establish a reasonable set of flavor-dependent distributions at an initial $Q_0^2$, motivated by physical constraints and data, then evolve to arbitrary $Q^2$ for use in predicting polarized observables. This approach is unique in many aspects. The distributions begin with information from the integrated distributions and impose normalization and positivity constraints (all flavors, valence and sea) to ensure that all of the spin information extracted from data is explicitly contained in the $x$-dependent results. We generate polarized parton distributions from the unpolarized distributions and well defined suitable assumptions, derived from the most recent polarized deep-inelastic-scattering (PDIS) data sets available [10–15].

For the polarized sea, we assume a broken SU(3) model, to account for mass effects in polarizing the sea. Our models separate out all flavors in the valence and sea for a complete analysis of the flavor dependence of the spin fractions in hadrons. We include charm via the evolution equations ($N_f$), at the appropriate $Q^2$ of charm production, to avoid any non-empirical assumptions about its size. The entire LO and NLO analysis is done in $x$-space. Physically, the small-$x$ behavior is of the Regge type, consistent with data and other theoretical approaches [2]. The large-$x$ behavior is compatible with the appropriate counting rules [16].

We consider three distinct models for the polarized gluons, which have a moderately wide range. Our choice effectively includes two separate factorization schemes: gauge invariant (GI) and chiral invariant (CI). These are all physically motivated models, whose overall size not large. The final parametrizations are easy to use, both in form and format. They are also in excellent agreement with the most recent data.

## II. THEORETICAL BACKGROUND

### A. Polarized quark distributions

Any distributions that are to be used to predict physical observables must be consistent with both existing, related

 

data and certain fundamental theoretical assumptions. In the case of the polarized distributions, the spin information as it applies to hadronic structure must be implicitly included, and the appropriate kinematic behavior must be explicit, so that they satisfy the fundamental constraints. This major requirement covers both the theoretical and experimental considerations which are important. Thus, we wish to construct the $x$-dependent polarized valence and sea quark distributions subject to the following physical constraints:

The integration over $x$ should reproduce the values extracted from PDIS data, so that the fraction of spin carried by each constituent is contained implicitly in the flavor-dependent distributions.

The distributions should reproduce the $x$-dependent polarized structure functions, $g_1^i$, $i=$p, n and d at the average $Q^2$ values of the data.

The small-$x$ behavior of $g_1(x)$ should fall between a Regge quark-like power of $x$ and a gluon-dominated logarithmic behavior.

The $Q^2$ behavior of the quark distributions should be consistent with the non-singlet and singlet next leading order (NLO) evolution equations, for the number of flavors appropriate to the $Q^2$ range to be covered.

The positivity constraints are satisfied for all of the flavors.

The first two constraints build in compatibility with both the integrated and the $x$-dependent polarized deep-inelastic-scattering (PDIS) data. The third and fourth conditions satisfy sound theoretical assumptions about both the $x$ and $Q^2$ kinematical dependence of the distributions. Finally, the last constraint is fundamental to our physical understanding of polarization.

#### *Valence and sea quark assumptions*

We construct the polarized valence distributions from the unpolarized distributions by imposing a modified SU(6) model [17,18]:

$$\Delta u_v(x) \equiv \cos\,\theta_D(x)\left[u_v(x)-\frac{2}{3}d_v(x)\right],$$

$$\Delta d_v(x) \equiv \cos\,\theta_D(x)\left[-\frac{1}{3}d_v(x)\right], \tag{2.1}$$

where the spin dilution factor is given by: $\cos\theta_D \equiv [1+R_0(1-x)^2/\sqrt{x}]^{-1}$. The $R_0$ term is chosen to satisfy the Bjorken sum rule (BSR), including the appropriate QCD corrections [19]. In the $Q^2$ region of the present PDIS data, we find that $R_0 \approx 2\alpha_s/3$. We may choose the unpolarized valence distributions $u_v$ and $d_v$ as either the Martin-Roberts-Stirling (MRS) set [20],

$$xu_v(x) = 2.43x^{0.6}(1-x)^{3.69}[1-1.18\sqrt{x}+6.18x],$$

$$xd_v(x) = 0.14x^{0.24}(1-x)^{4.43}[1+5.63\sqrt{x}+25.5x], \tag{2.2}$$

or the CTEQ [21] set,

$$xu_v(x) = 1.344x^{0.501}(1-x)^{3.689} \times [1+6.402x^{0.873}],$$

$$xd_v(x) = 0.640x^{0.501}(1-x)^{4.247} \times [1+2.690x^{0.333}], \tag{2.3}$$

or equivalent.

If we assume a model of the sea obtaining its polarization from gluon bremsstrahlung, then the polarized distributions naively would have a form $\Delta q_f = x q_f$ [22,23]. However, the polarized deep-inelastic scattering data appear to imply a negatively polarized sea [1]. If the integrated structure functions are to agree with data, then the normalization defined by $\eta_{av} \equiv \langle \Delta q \rangle / \langle xq \rangle$ must be a part of the proportionality between the polarized and unpolarized distributions. Meanwhile, the positivity constraint, which requires $|\Delta q| \leqslant q$ for all $x$, implies a functional form for the function $\eta(x)$. The basic idea of the bremsstrahlung model, coupled with the implications of the data motivate the following form for the flavor dependent polarized sea distributions:

$$\Delta q_f(x) \equiv \eta_f(x) x q_f(x), \tag{2.4}$$

where $q(x)$ is the $x$-dependent unpolarized distribution for flavor $f$. The function $\eta(x)$ is chosen to satisfy the normalization constraint

$$\langle \Delta q_f \rangle = \int_0^1 \eta_f(x) x q_f(x) dx \equiv \langle \eta x q_f \rangle = \eta_{av} \langle x q_f \rangle, \tag{2.5}$$

where $\eta_{av}$ is extracted from data for each flavor [1]. Physically, $\eta(x)$ may be interpreted as a modification of $\Delta q$ due to unknown effects of soft physics at low $x$. This motivates a form for $\eta(x)$, which will be discussed later.

#### *Positivity constraint*

For the purposes of this analysis, we are assuming that the sea quarks are effectively massless, so each quark has a definite helicity state. In essence, this ignores higher twist transverse spin effects in the entire kinematic range considered. Thus, there is a probabilistic interpretation of the parton densities, q, and the net parton distribution is given by: $q = q\uparrow + q\downarrow$. The total polarization is given as the difference of probabilities of finding polarized $\uparrow$ and $\downarrow$ partons in the nucleon: $\Delta q \equiv q\uparrow - q\downarrow$. In a polarized $\uparrow$ proton, this probability for sea quarks should be less than that of the total unpolarized sea distribution, since every quark is in a given helicity state. This is the positivity constraint: i.e,

$$|\Delta q(x)| \leqslant q(x) \tag{2.6}$$

for all $x$.

This is valid for the leading order (LO) $x$-dependent distributions which have a clear probabilistic interpretation, because there is no intrinsic scheme dependence at this level. The results in the next-to-leading-order (NLO) treatment depend only upon the Gribov-Lipatov-Altarelli-Parisi (GLAP)

evolution, so there is no problem with constraining the sea quarks using positivity at $Q_0^2$ in either case. The valence quarks satisfy the positivity constraint by construction. Although the probabilistic meaning gives rise to the positivity constraint, it is not clear what role the chiral and gauge invariant schemes have on this interpretation. In our treatment, the polarized gluon distribution is assumed small at these low $Q^2$ values, so the schemes are close enough so that positivity is unaffected. This provides a motivation to choose a zero $\Delta G$ model—to investigate the gauge invariant factorization.

#### *Evolution*

The polarized partons are grouped in a linear combination which is a singlet of flavor $SU_f(3)$ group and a nonsinglet linear combination of that group. The singlet/non-singlet designations are useful for delineating certain evolution and factorization properties of the quarks. These combinations can be related to the usual flavor decomposition, including the valence, sea and gluons. The nonsinglet term $\Delta q_{NS}$ is a linear combination of the triplet $a_3$ axial charge and an octet $a_8$ axial charge of the $SU_f(3)$ symmetry. The singlet, $\Delta\Sigma$ is related to the axial charge, $a_0$ and is normally associated with the axial anomaly, which includes a gluonic contribution. This depends upon the factorization scheme, which will be discussed shortly.

The non-singlet term is dominated by the valence distribution, under polarized ($\Delta u_s$, $\Delta d_s$) symmetry. Its first moment is scale ($Q^2$) independent in LO. The singlet term has a definite physical interpretation in the gauge invariant scheme, even though it is scale dependent. Since we are going to assume a small $\Delta G$ in all of our models, this interpretation will be essentially valid, even in the chiral invariant (Adler-Bardeen) scheme, which separates out the anomaly. In both cases, our distributions are constructed within the positivity constraint. In the NLO analysis, the initial distributions are constructed at $Q_0^2=1.0$ GeV$^2$, where they satisfy the constraints that we have set. We assume that higher-twist effects are negligible compared to the quantities used to determine our distributions at this value of $Q_0^2$ [24]. The distributions are then evolved in NLO, completely independent of any further considerations. In the evolution, the separation of singlet and non-singlet is faithfully maintained. Thus, we can satisfy all of the important physical constraints.

Our parton distributions are evolved directly in $x$-space using an iteration technique first suggested in [25] and we use the splitting functions recently calculated in [26]. This method requires less computer time than the ''brute force'' technique recently used in [27] and it eliminates the need to invert from $n$-moment space using the conventional evolution techniques. One advantage of our technique is that it avoids the need to know the *measured* structure function over the whole $x$-region, i.e., from $x=0$ to $x=1$, which is necessary if one is to extract Mellin moments from the data [28]. Details of the technique can be found in [29].

### B. The role of polarized gluons

#### *Factorization*

In PDIS, there are two factorization schemes which can be used to represent the polarized sea distributions: the gauge-invariant [30] [or modified minimal subtraction (MS)] and the chiral invariant [31] (or Adler-Bardeen) schemes [32]. In the chiral-invariant (AB) scheme, the axial gluon anomaly term [33], which depends upon the polarized gluon distribution, is separated out from the chiral invariant polarized quark distributions. Since the measured distributions must be gauge invariant, the relation between the two scheme dependent distributions is

$$\Delta q(x)_{GI}=\Delta q(x)_{CI}-\frac{N_f\alpha_s}{2\pi}\Delta G, \tag{2.7}$$

where the GI refers to the gauge-invariant scheme and CI to the chiral-invariant scheme. Thus, the size of $\Delta G$ is relevant in the CI scheme. This, in turn, affects the average $\eta$ values extracted for each flavor. Thus, $\Delta G$ has an indirect bearing on the polarized sea distributions [1].

There exists no empirical evidence that the polarized gluon distribution is very large at the relatively small $Q^2$ values of the data. In fact, even in the NLO evolution, the polarized gluon distribution does not evolve significantly between $Q^2=1$ and $Q^2=10$ GeV$^2$, regardless of which model is chosen. Data from Fermilab [34] indicate that it is likely small at the $Q^2$ values of existing data. In addition, a theoretical model of the polarized glue, based on counting rules, implies that $\Delta G\approx\frac{1}{2}$ [16]. Other theoretical models substantiate this claim, as well [35,36]. However, since we do not know the explicit size of the $\Delta G$ in this kinematic region, we perform our analysis using three distinct physical models. The evolution of $\Delta G$ is then done both in LO and NLO to investigate any possible NLO effects.

The first set of $\eta(x)$ functions, quoted in Table I, assumes a moderately polarized glue:

$$\Delta G(x)=xG(x)=31.3x^{0.41}(1-x)^{6.54}[1-4.64\sqrt{x}+6.55x], \tag{2.8}$$

using an unpolarized MRS glue, normalized to 0.50 or

$$\Delta G(x)=xG(x)$$
$$=1.123x^{-0.206}(1-x)^{4.673}[1+4.269x^{1.508}], \tag{2.9}$$

for the CTEQ gluon distribution, consistent with the analysis in [1].

For the second polarized gluon model, we set $\Delta G=0$ to determine $\eta_{av}$ and parametrize the $\eta(x)$ accordingly. This is equivalent to the gauge-invariant scheme, since the anomaly term vanishes. Any analysis which requires a gauge-independent set of flavor dependent distributions (such as on the lattice) should use this set of polarized distributions at $Q_0^2$, evolved to the appropriate $Q^2$ values. The corresponding $\eta(x)$ functions are listed in Table II.

The third gluon model is motivated by an instanton-induced polarized gluon distribution, which gives a negatively polarized glue at small-$x$ [37]. This modified distribution (normalized to $\Delta G=-0.23$) is given by the best fit to the curve in [37]:

$$\Delta G(x)=7(1-x)^7[1+0.474\ \ln(x)]. \tag{2.10}$$

This would allow for instanton based non-perturbative effects at small $Q^2$.

#### *Relation between the sea and glue in $g_1$*

The valence polarizations are rather well established from the BSR and the polarized DIS experiments. The valence quarks are dominant at large $x$ and they give their polarization to the gluons through bremsstrahlung, which in turn, creates sea polarization via pair-production. But the sea quarks share the momentum from the gluon which created the pair, and thus, each constituent is at lower $x$ than the original valence ''parent.'' This is consistent with the polarized sea being dominant at lower $x$. The PDIS data imply that the sea is polarized opposite to that of the valence quarks. The relative size of the negative sea polarization is an indication as to whether gluon polarization is moderately positive (such as $\Delta G = xG$, implying that polarization of G carries most of the spin of the proton), nil, or negative. We expect a larger negatively polarized sea for the last two cases as it must offset the positive anomaly term proportional to gluons in the chiral-invariant scheme and the $J_z = \frac{1}{2}$ sum rule in either scheme. If the polarized sea is smaller (less negative) or the polarized gluon is large, the $g_1^p$ curve will exhibit a sharper rise at small $x$. When future data are available with smaller error bars, these scenarios can be better defined to yield the correct sign and size of $\Delta G$. There may be a possibility to argue a positive proportionality of spin and momentum of the sea if $\Delta G$ is very large. A much larger polarized gluon distribution can imply either a smaller negatively polarized sea or even a slightly positive polarized sea. However, this would require a prohibitively large polarized glue at these smaller $Q^2$ values. We argue that this is not likely for the following reasons:

(1) When the light-cone wave functions at small-$x$ are analyzed, they implicate a negatively polarized sea [38].

(2) In order for the sea to be entirely positive, $\Delta G$ would have to be prohibitively large to satisfy the data. The orbital angular momentum would have to be correspondingly large to satisfy the J=1/2 sum rule. This would also disagree with the implications of the E704 data [34].

(3) Our highly successful fits to the $x$-dependent data not only indicate that $\Delta G$ is likely moderate at $Q^2 = 10\ \mathrm{GeV}^2$, but that the data at lower $Q^2$ is fit somewhat better with even smaller $\Delta G$. This is consistent with the evolution of the polarized gluon distribution. We also show in Sec. IV that the growth of $\Delta G$ presented by ABFR [4] is not likely, even in NLO. Thus, our present analysis further strengthens the point of a smaller $\Delta G$ at these lower $Q^2$ values.

(4) Most all other independent analyses agree with the negatively polarized sea.

We conclude that a positively polarized sea and a very large $\Delta G$ seem unlikely, given present data.

### C. Extrapolation of data to small-$x$

Extrapolation of $g_1^i$ $(i = p,n,d)$ to small-$x$ is important experimentally for determination of the integrated values of these structure functions. Theoretically, the $g_1$ behavior at small-$x$ is important to understanding the mechanisms which underlie the physics in this region. There are various models that attempt to explain the contributions to both $F_2$ and $g_1$ at low-$x$. The data appear to exhibit growth of these quantities, but since the error bars are somewhat large, most of the predicted types of behavior cannot be ruled out [39].

At large-$x$, the valence distributions dominate $F_2$ and $g_1$ and these are more well determined than the sea distributions, which are more prevalent at small-$x$. Thus, one must make suitable assumptions about the behavior of the polarized sea at low-$x$. Experimental analyses [14,12] have tended to assume a relatively constant behavior and extrapolate $g_1$ from its value at about $x \sim 10^{-2}$ down to $x = 0$. A model by Donnachie and Landshoff [40] assumes that the Pomeron couples via vector $\gamma_\mu$ so that $g_1$ exhibits a logarithmic behavior: $g_1 \sim \ln(1/x)$. Bass and Landshoff [41] analyze a model of a two-gluon Pomeron which leads to a slightly more divergent behavior at small-$x$: $g_1 \sim [1 + 2\ln(x)]$. If negative parity Pomeron cuts contribute to the spin-dependent cross section, a divergent behavior of $g_1$ results [42], corresponding to the singular form: $g_1 \sim 1/x\ \ln^2(x)$.

We make no presumptions about the forms of the flavor dependent distributions at small-$x$, other than their relation to the unpolarized distributions. The parametrization of $\eta_f(x)$ in Eq. (2.4) will be determined primarily from normalization and positivity constraints. Once the polarized sea flavors are generated, we can determine resulting the small-$x$ behavior of $g_1$ and compare it to these theoretical models.

## III. PHENOMENOLOGY

### A. Polarized quark flavors

In the work of [1], the integrated polarized structure functions were compared to the spin averaged distributions, to establish a comparison between the spin and momentum carried by each flavor of quark. The results indicate that the relation is flavor dependent, but the magnitudes of these ratios [$\eta_{av}$ in Eq. (2.5)] are of the same order of magnitude. Although this does not necessarily imply that there is a direct relation between the two, it does provide a suitable starting point for generating the polarized distributions from known unpolarized distributions, which satisfy the data on spin-averaged physical processes. This is the motivation for the form in Eq. (2.4) for the polarized flavor-dependent distributions. The integrated data are satisfied by choosing the parameters in $\eta(x)$ to satisfy Eq. (2.5) and the positivity constraints. We also wish to stay consistent with counting rules at large-$x$ [16]. The small-$x$ behavior can be controlled by the functional form that we choose for $\eta(x)$. All of these constraints are to be satisfied at some low value of $Q^2$, and the evolution equations will ensure that positivity and the kinematical behavior stay consistent at all $Q^2$.

A possible form for $\eta(x)$, which gives flexibility in satisfying the constraints (2.5) and (2.6) is $\eta(x) = a + bx^n$. We expect the function to be decreasing with $x$, since the problems with positivity (for $|\eta_{av}| > 1$) occur at large $x$. We

chose not to modify the $(1-x)$ dependence in order to keep the counting rule powers in tact (insofar as the unpolarized distributions do this) for the large-$x$ behavior. We were able to satisfy the positivity constraint at all $x$ using this form for $\eta(x)$.

In the following analysis, we assume the unpolarized distributions in the CTEQ form: $q(x)=A_0x^{A_1}(1-x)^{A_2}(1+A_3x^{A_4})$. Then, using Eq. (2.4), we generate the corresponding polarized distributions for each flavor. An analysis with the MRS distributions yields similar results.

For the CTEQ distributions, we have

$$x\overline{q}(x)=\frac{1}{2}[0.255x^{-0.143}(1-x)^{8.041}(1+6.112x) \mp 0.071x^{0.501}(1-x)^{8.041}], \tag{3.1}$$

where the $(-)$ holds for $\overline{u}$ and the $(+)$ for the $\overline{d}$ flavors. The strange sea has the parametrization

$$x\overline{s}(x)=[0.064x^{-0.143}(1-x)^{8.041} \times(1+6.112x)]. \tag{3.2}$$

Both of these sets account for the $\overline{u}$, $\overline{d}$ asymmetry in the unpolarized sea.

The corresponding integrated polarized distributions can be written in terms of beta functions, $B(m,n)$, as

$$\begin{aligned}\langle\Delta q\rangle=&aA_0B(A_1+2,A_2+1)\\&+aA_0A_3B(A_1+A_4+2,A_2+1)\\&-bA_0B(A_1+n+2,A_2+1)\\&-bA_0A_3B(A_1+A_4+n+2,A_2+1)\end{aligned} \tag{3.3}$$

for the CTEQ distributions. The integral $\langle xq\rangle$ can be similarly written and thus the restriction on $a$ and $b$, corresponding to the normalization constraint (2.5) is $a=\eta_{av}-b\lambda$, where

$$\lambda\equiv\frac{B(A_1+n+2,A_2+1)+A_3B(A_1+A_4+n+2,A_2+1)}{B(A_1+2,A_2+1)+A_3B(A_1+A_4+2,A_2+1)}, \tag{3.4}$$

for the CTEQ unpolarized distributions.

The positivity constraint in terms of $a$ and $b$ is

$$\frac{|\Delta q(x)|}{q(x)}=|ax+bx^{n+1}|\leq 1, \tag{3.5}$$

for all $x\in[0,1]$. In the following discussion, we will show how $\eta(x)$ is generated for the zero polarized gluon case. The procedure is virtually identical to the other two gluon models where the anomaly term is present.

When we choose $a$ to satisfy the normalization constraint (2.5) and $b$ to satisfy the positivity constraint (2.6), the $x$-dependent polarized distribution for each flavor is determined from (2.4). These conditions are independent of the set of unpolarized distributions that is used. However, one must be consistent by using the appropriate set of unpolarized distributions which were used to determine the function $\eta(x)$. Therefore, we seek the form

$$\eta(x)=(\eta_{av}-b\lambda)+bx^n, \tag{3.6}$$

where both $b$ and $n$ are chosen to satisfy the positivity constraint (3.5). This form of $\eta(x)$ is motivated by (1) associating this function with modifications of $\Delta q$ by small-$x$ physics and (2) keeping the $(1-x)$ dependence in tact to be consistent with counting rule behavior at large $x$ to the extent that the unpolarized distributions have this desired form [16]. We can then both satisfy positivity (even at large $x$) and control the small $x$ behavior, where the sea and glue are most prominent.

#### *Choice of $\eta(x)$ at small-x*

The polarized sea and the gluon distributions are expected to dominate in the small-$x$ region. If we assume a strongly polarized negative sea, with $\eta_{av}<-1$ then this defines a range of $b$ values which satisfy the positivity constraint. The behavior of our ansatz $\eta(x)=a+bx^n$ for $0<n<1$ is suited for small-$x$ dependence. When a certain small-$x$ behavior is desired, a series of $n$ values can be tried for the best fits to data. In fact, when $0.2<n<1.0$, it is easier to satisfy both constraints with appropriate choices of $a$ and $b$. These values of $n$ allow a wider range of $a$ and $b$ values. However, when $0<n<0.2$, the range of possible $a$ and $b$ values which satisfy the constraints gets very small and will not be the same for all experimental yields of $\eta_{av}$. Thus, it makes it impossible to find a uniform fit for $\eta(x)$ for each flavor. Since $\eta(x)$ should be only flavor dependent to have any physical connection, we must choose $n$ so that $a$ and $b$ will be comparable for all experimental results.

TABLE I. $\eta$ Values from data and $\eta(x)$: $\Delta G=xG$.

| Quantity | $\eta_{u,d}$ | $\eta_s$ | $\eta_u(x)$ | $\eta_s(x)$ |
|---|---|---|---|---|
| $SMC(I^p)$ | $-2.0$ | $-1.6$ | $-2.84+2.8\sqrt{x}$ | $-2.23+2.1\sqrt{x}$ |
| $E143(I^p)$ | $-1.8$ | $-1.2$ | $-2.64+2.8\sqrt{x}$ | $-1.83+2.1\sqrt{x}$ |
| $E154(I^n)$ | $-1.5$ | $-0.6$ | $-2.34+2.8\sqrt{x}$ | $-1.23+2.1\sqrt{x}$ |
| $HERMES(I^n)$ | $-1.3$ | $-0.3$ | $-2.14+2.8\sqrt{x}$ | $-0.93+2.1\sqrt{x}$ |
| $E143(I^d)$ | $-1.6$ | $-0.8$ | $-2.44+2.8\sqrt{x}$ | $-1.43+2.1\sqrt{x}$ |
| $SMC(I^d)$ | $-2.4$ | $-2.3$ | $-3.24+2.8\sqrt{x}$ | $-2.93+2.1\sqrt{x}$ |

TABLE II. $\eta$ values from data and $\eta(x)$: $\Delta G=0$.

| Quantity | $\eta_{u,d}$ | $\eta_s$ | $\eta_u(x)$ | $\eta_s(x)$ |
|---|---|---|---|---|
| $SMC(I^p)$ | $-2.4$ | $-2.2$ | $-3.30+3.0\sqrt{x}$ | $-3.09+2.9\sqrt{x}$ |
| $E143(I^p)$ | $-2.2$ | $-2.0$ | $-3.10+3.0\sqrt{x}$ | $-2.87+2.9\sqrt{x}$ |
| $E154(I^n)$ | $-1.8$ | $-1.3$ | $-2.70+3.0\sqrt{x}$ | $-2.17+2.9\sqrt{x}$ |
| $HERMES(I^n)$ | $-1.7$ | $-1.0$ | $-2.60+3.0\sqrt{x}$ | $-1.90+2.9\sqrt{x}$ |
| $E143(I^d)$ | $-2.0$ | $-1.6$ | $-2.90+3.0\sqrt{x}$ | $-2.47+2.9\sqrt{x}$ |
| $SMC(I^d)$ | $-2.7$ | $-2.9$ | $-3.60+3.0\sqrt{x}$ | $-3.77+2.9\sqrt{x}$ |

TABLE III. $\eta$ values from data and $\eta(x)$: Neg. $\Delta G$.

| Quantity | $\eta_{u,d}$ | $\eta_s$ | $\eta_u(x)$ | $\eta_s(x)$ |
|---|---|---|---|---|
| $SMC(I^p)$ | $-2.5$ | $-2.5$ | $-3.43+3.1\sqrt{x}$ | $-3.49+3.3\sqrt{x}$ |
| $E143(I^p)$ | $-2.4$ | $-2.4$ | $-3.33+3.1\sqrt{x}$ | $-3.39+3.3\sqrt{x}$ |
| $E154(I^n)$ | $-2.0$ | $-1.7$ | $-2.93+3.1\sqrt{x}$ | $-2.99+3.3\sqrt{x}$ |
| $HERMES(I^n)$ | $-1.9$ | $-1.5$ | $-2.83+3.1\sqrt{x}$ | $-2.89+3.3\sqrt{x}$ |
| $E143(I^d)$ | $-2.2$ | $-2.0$ | $-3.13+3.1\sqrt{x}$ | $-3.19+3.3\sqrt{x}$ |
| $SMC(I^d)$ | $-2.9$ | $-3.2$ | $-3.83+3.1\sqrt{x}$ | $-3.89+3.3\sqrt{x}$ |

Positivity of $n$ is, in principle, not essential. If we choose a small negative $n$, we enhance the divergence of $g_1$ as $x \to 0$. This favors strong anti-polarization of sea at small-$x$ and could give the sea some positive polarization for large $x$. However, it is virtually impossible to satisfy both the normalization and positivity constraints simultaneously with negative $n$ and such a simple parametrization of $\eta$. Thus, it does not appear to be advantageous to choose $n$ to be negative, especially since we have fit the data successfully with $n=\frac{1}{2}$.

The ranges for possible $\eta(x)$ functions are given in Tables I through III. The corresponding polarized distributions satisfy the DIS data and the positivity constraint.

### B. Input from DIS data

In Tables I through III, we summarize the integrated results for each considered experiment, with the values for $\eta_{av}$ in each gluon model. The corresponding functional form for each $\eta(x)$ is shown, which satisfies the constraints discussed in the text. We chose two sets of data each, for the proton [10,14], neutron [11,13] and deuteron [10,14]. These represent the latest published data and are representative of the groups at SLAC, CERN and DESY.

Since our ultimate goal is to find a suitable set of flavor-dependent $\eta(x)$ functions, which do not depend upon a specific experimental result, we take a suitable average of $\eta(x)$ for each flavor to generate the polarized sea quark distributions. There is enough flexibility in the choice of $a$ and $b$, given the experimental errors and the range of values which satisfy positivity, so that all constraints are still satisfied. Note from the tables that the range of $a$ values is not considerable, even when the values of $b$ are fixed. Our choice of the averaging procedure is further justified by our ability to reproduce the data from all of the experiments. The resulting functions $\eta(x)$ for each gluon model are

| *Quantity* | $\eta_{u,d}(x)$ | $\eta_s(x)$ |
|---|---|---|
| $\Delta G = xG$ | $-2.49+2.8\sqrt{x}$ | $-1.67+2.1\sqrt{x}$ |
| $\Delta G = 0$ | $-3.03+3.0\sqrt{x}$ | $-2.71+2.9\sqrt{x}$ |
| $\Delta G < 0$ | $-3.25+3.1\sqrt{x}$ | $-3.31+3.3\sqrt{x}$ |

## IV. RESULTS AND DISCUSSION

### A. Results for the polarized distributions

The polarized valence quark distributions are constructed with the assumptions made in Eqs. (2.1) and (2.3), with $R_0$ determined by the BSR. The overall parametrization for each of the polarized sea flavors, including the $\eta(x)$ functions, the anomaly terms and the up-down unpolarized asymmetry term can be written (with the CTEQ basis) in the form:

$$\Delta q_i(x) = -A x^{-0.143}(1-x)^{8.041}(1-B\sqrt{x}) \times [1+6.112x+P(x)]. \tag{4.1}$$

The values for the variables in Eq. (4.1) are given for each flavor and each gluon model at $Q_0^2 = 1.0$ GeV$^2$ in Table IV.

We have used these to calculate the polarized structure functions, $xg_1(x)$, for the proton, neutron and deuteron. These are all compared with the corresponding data at the average $Q^2$ value for that data set. These plots are shown in Figs. 1 through 4. In these figures, the solid line corresponds to the small polarized gluon model, the dashed line to the zero polarized glue and the dotted lines to the instanton motivated gluon model.

TABLE IV. Parametrizations for polarized sea flavors at $Q_0^2 = 1.0$ GeV$^2$.

| Flavor | $\Delta G$ | $A$ | $B$ | $P(x)$ |
|---|---|---|---|---|
| $\langle \Delta u \rangle_{sea}$ | $xG$ | 0.317 | 1.124 | $-0.278x^{0.644}-1.682x^{0.937}(1-x)^{-3.368}(1+4.269x^{1.508})$ |
| $\langle \Delta d \rangle_{sea}$ | $xG$ | 0.317 | 1.124 | $+0.278x^{0.644}-1.682x^{0.937}(1-x)^{-3.368}(1+4.269x^{1.508})$ |
| $\langle \Delta s \rangle$ | $xG$ | 0.107 | 1.257 | $-3.351x^{0.937}(1-x)^{-3.368}(1+4.269x^{1.508})$ |
| $\langle \Delta u \rangle_{sea}$ | 0 | 0.386 | 0.990 | $-0.278x^{0.644}$ |
| $\langle \Delta d \rangle_{sea}$ | 0 | 0.386 | 0.990 | $+0.278x^{0.644}$ |
| $\langle \Delta s \rangle$ | 0 | 0.173 | 1.070 | 0 |
| $\langle \Delta u \rangle_{sea}$ | *Neg* | 0.414 | 0.954 | $-0.278x^{0.644}-10.49x^{1.143}(1-x)^{-1.041}(1+0.474\ \ln x)$ |
| $\langle \Delta d \rangle_{sea}$ | *Neg* | 0.414 | 0.954 | $+0.278x^{0.644}-10.49x^{1.143}(1-x)^{-1.041}(1+0.474\ \ln x)$ |
| $\langle \Delta s \rangle$ | *Neg* | 0.212 | 0.997 | $-20.89x^{1.143}(1-x)^{-1.041}(1+0.474\ \ln x)$ |

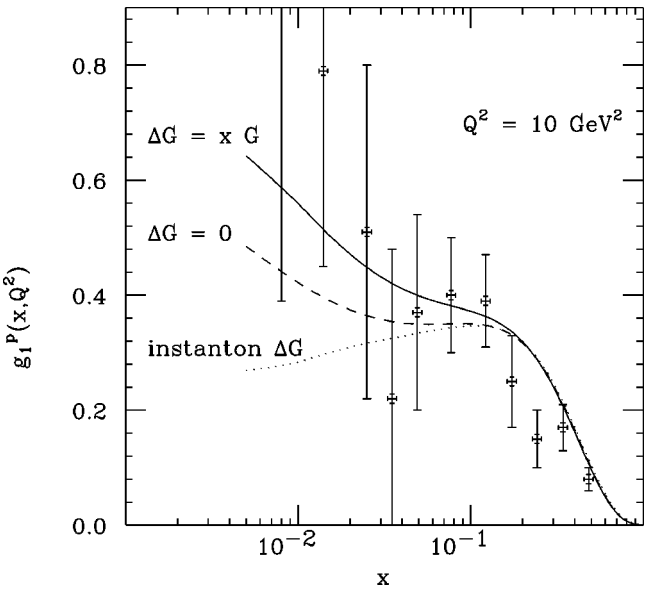


FIG. 1. The polarized proton structure $g_1^p$ as a function of $x$ at fixed $Q^2$ for three models of $\Delta G$ compared to data, and highlighting small $x$ behavior.

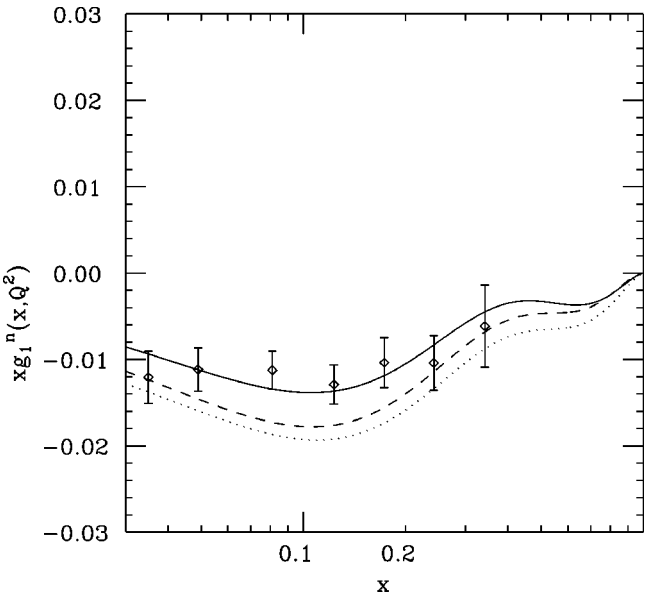


FIG. 3. The polarized neutron distribution $xg_1^n$ as a function of $x$ at $Q^2=10$ GeV$^2$ compared to data. The three curves are for three different gluon models (see text).

In order to verify that our models for $\Delta G$ were reasonable, considering that the evolution governs the $Q^2$ behavior of the distributions, we evolved $\Delta G(x,Q_0^2=1)$ to $Q^2=1000$ GeV$^2$ for each model using both LO and NLO singlet evolution. The $x$-behavior of the gluon distributions is shown in Figs. 5 through 7 at the appropriate orders of magnitude of $Q^2$. The corresponding integrated values for these evolved distributions are shown in Tables V and VI.

For comparison with other models of the polarized quarks, we show the $x$-dependent distributions of the valence and sea for each flavor in Figs. 8–11. The sea flavors are shown for each gluon model. Note that our results compare favorably with other models. There seems to be a general agreement about the shape of these distributions. Differences arise in the actual numerical values of the integrated distributions. Both our $x$-dependent and our integrated distributions have been constructed to satisfy all of the present data.

***Physics implications***

(1) All comparisons of our distributions with existing data are excellent, including Fig. 1, which shows $g_1$, as opposed to $xg_1$, accentuating the small-$x$ behavior. The best overall fits occur with the moderate glue (model 1). The zero glue model results are somewhat better for the neutron, where the

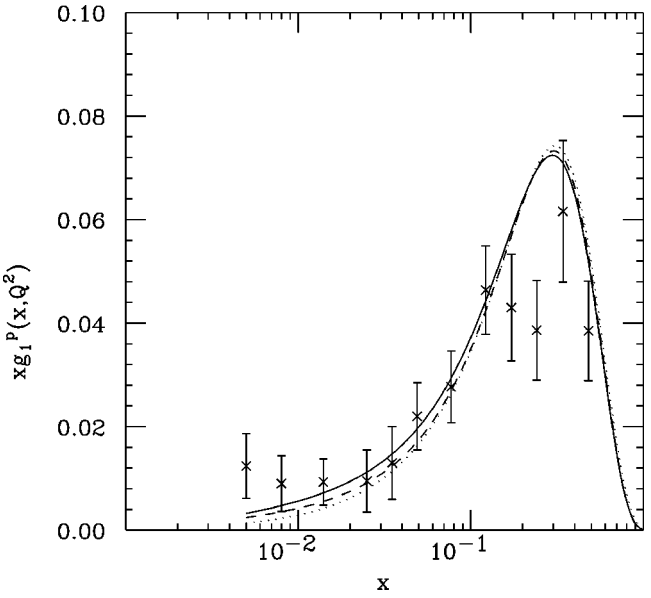


FIG. 2. Same as Fig. 1 but for $xg_1^p$ highlighting medium $x$ behavior.

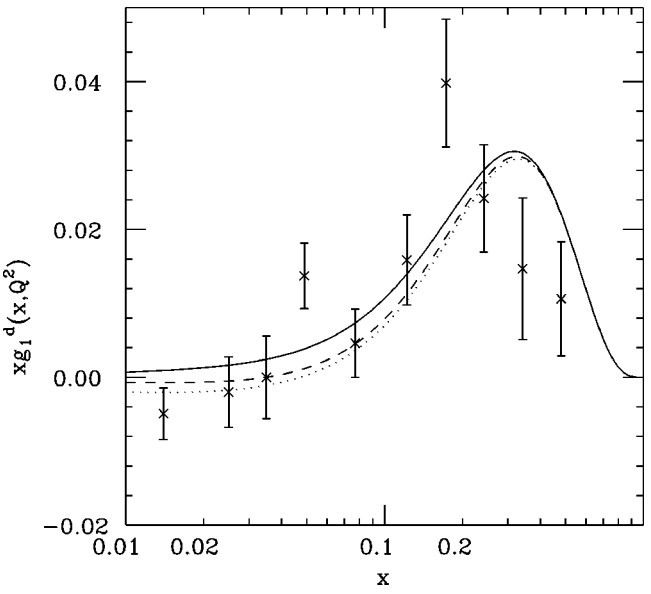


FIG. 4. Same as Fig. 3 for $g_1^d$.

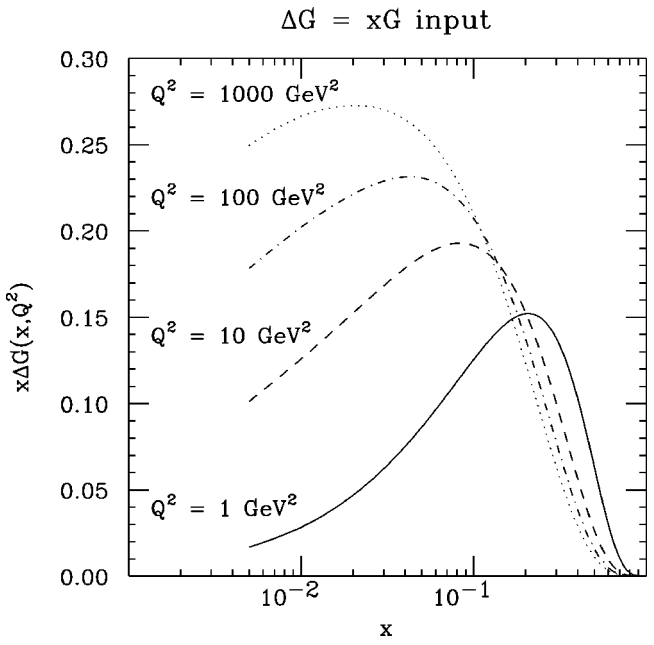


FIG. 5. Polarized gluon distribution as a function of $x$ at different $Q^2$ values for the $\Delta G = xG$ input.

data are at lower average $Q^2$ values. This is consistent with the $Q^2$ evolution of the polarized gluon distribution.

(2) At small-$x$, the instanton gluon model predicts that $g_1^p$ decreases slightly. However, considering the latitude in this distribution, it is consistent with a constant behavior. The data appear to be rising in this $x$ region, contrary to this implication. Since the data are at average $Q^2$ of 10 GeV$^2$, this seems to indicate that the gluons are not negatively polarized at such a relatively large $Q^2$. This is consistent with the assumption that instantons are dominant at smaller $x$ and $Q^2$ values and are likely not a major contributor to the polarized glue at higher $Q^2$ [37].

(3) The polarized gluon distribution does not evolve as large as BFR predict [4], even with the moderate gluon model. Assumption of such large polarization at these lower $Q^2$ values is unfounded. In fact, data from E704 at Fermilab indicate that it is likely more on the order of the moderate or zero distribution. Even the NLO integrated polarized gluons do not evolve significantly different from the LO distributions.

(4) Our up and down valence distributions are comparable to others. Ours is motivated from the physical SU(6) model with the BSR fixing the lone free parameter. It is compatible with the u-valence domination at large $x$ and has the appropriate $x$-dependent behavior at all other $x$ values.

(5) The u and d polarized sea distributions are not highly dependent on the gluon model used to generate them. However, the polarized strange sea is quite sensitive to the gluon model and hence the anomaly term. This is discussed in more detail in [1].

(6) The shape of the $x$-dependent polarized sea distributions agrees with the analysis of Antonuccio *et al.* [38]. They exhibit Regge-like behavior at small-$x$ and become slightly positive at moderate $x$. Although it is not completely obvious from the figures, our sea distributions remain negative until about $x \sim 0.3$ and then turn slightly positive. This is hidden by the dominance of the valence quarks in this kinematic range, but indicates a consistency with physical expectations of the polarized sea.

### B. Small-$x$ behavior

For the SMC proton data with the CTEQ unpolarized distributions and the positive gluon model, we find at small $x$ that: $g_1^p \sim x^{-0.19}$. Phenomenologically, this is due to the interplay between the sea distributions, with a $\Delta q_i \sim x^{-0.143}$ behavior in Eq. (3.1) and the gluons in the model, dominated by $xG \sim x^{-0.206}$ at small-$x$ in Eq. (2.9). Physically, this is consistent with Regge behavior, characteristic of the isotriplet contributions to $g_1$. It does not have the steep rise characteristic of the singlet behavior due to gluon exchange, but is slightly steeper than the quoted Regge intercept [43]. This could either be due to the uncertainty in the value of the Regge intercept [44] or to an interplay between the quarks and the logarithmic gluon exchange [41]. This gluon-sea interplay is also seen in the other polarized gluon models, where the smaller (and negative) $\Delta G$ moderate the rise is $g_1^p$.

Extrapolating our results in Fig. 1 to $x = 0.002$, we can compare to some of the models of small-$x$ behavior discussed in Sec. II. Our moderate gluon model would give $g_1^p$ a value of about 0.75 here, which is steeper than the $A_1$ intercept of $-0.14$ for the isotriplet piece, but not as steep as the two-gluon model of the Pomeron. It is, however, consistent with the vector coupling model of Donnachie and Landshoff. The zero polarized gluon model gives $g_1^p$ a slightly less steep slope, but is also consistent with this model. Here, the polarized sea dominates $g_1^p$ at small-$x$. The instanton-motivated gluon model creates a relatively constant behavior for $g_1^p$.

In our treatment, the polarized sea dominates the quark contribution at small-$x$. Since our basic assumption is $\Delta q/q \sim x$ it follows that $A_1(x) \sim x$. Therefore, the relation $g_1(x) \approx F_2(x) A_1(x)/2x(1+R)$ implies that $F_2$ and $g_1$ have the same behavior at small $x$. The instanton motivated gluon model gives a constant $g_1^p$ behavior, which seems to disagree with the apparent rise in $F_2$ and, correspondingly, $g_1$. Thus, the small-$x$ behavior of the data are not consistent with the negative $\Delta G$ model. It may therefore be possible to rule out negative $\Delta G$ at these $Q^2$ values if the error bars on $g_1$ can be reduced in future PDIS experiments. This does not address the possibility for negative $\Delta G$ at smaller $Q^2$, where non-

TABLE V. Leading order polarized gluon evolution: $\int_{x_{min}}^1 \Delta G dx$.

| $Q^2$(GeV$^2$) | $\Delta G = xG$ | $\Delta G = 0$ | *Instanton* |
|---|---|---|---|
| 1 | 0.387 | 0.071 | $-0.076$ |
| 10 | 0.651 | 0.107 | $+0.045$ |
| 100 | 0.736 | 0.167 | $+0.118$ |
| 1000 | 0.794 | 0.211 | $+0.182$ |

TABLE VI. Next-to-leading order polarized gluon evolution: $\int_{x_{min}}^{1} \Delta G dx$.

| $Q^2(\mathrm{GeV}^2)$ | $\Delta G = xG$ | $\Delta G = 0$ | *Instanton* |
|---|---|---|---|
| 1 | 0.424 | 0.080 | −0.082 |
| 10 | 0.653 | 0.119 | +0.047 |
| 100 | 0.751 | 0.183 | +0.130 |
| 1000 | 0.811 | 0.229 | +0.190 |

perturbative effects are present.

The neutron and deuteron structure functions appear to have more moderate behavior at small-$x$ (see Figs. 3 and 4). In fact, $g_1^d$ asymptotically approaches zero, to within experimental errors. Since it is not clear whether $g_1^n$ is negatively increasing or tending to zero, we cannot conclude whether there are cancellations of $g_1^p$ and $g_1^n$ at small-$x$ to give this moderate behavior to $g_1^d$ or whether other nuclear effects could be present. Similarly, we cannot distinguish between the gluon models with these data, as readily as the proton case. All of the moderate gluon models seem to fit the data fairly well. A much larger $\Delta G$ would not provide good agreement at low-$x$. More precise data at small-$x$ could yield more exact conclusions.

## V. CONCLUDING REMARKS

We have constructed a set of flavor-dependent polarized parton distributions using QCD motivated assumptions and recent PDIS data. The main advantages of our approach are that: both the gauge-invariant (GI) and chiral-invariant (CI) factorization are included, the positivity constraint holds for all flavors and the parametrizations include valence quarks and all light flavors of the sea, in a form is easy to implement for predicting polarized processes.

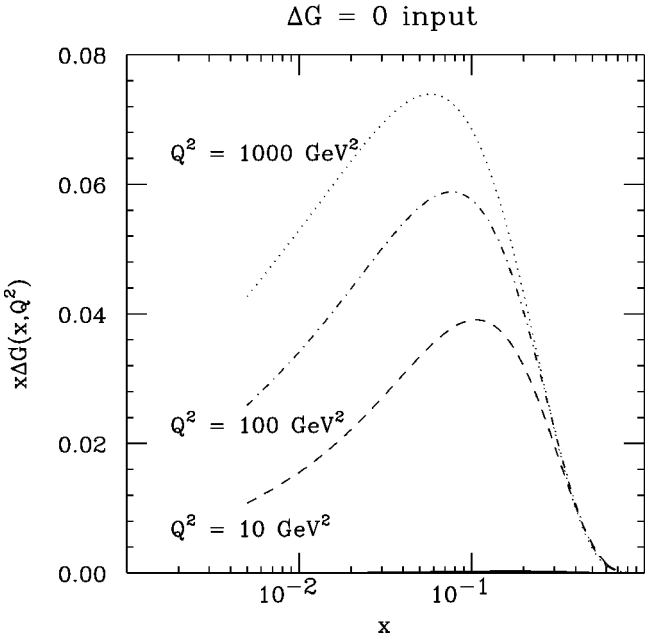


FIG. 6. Same as Fig. 5 for the $\Delta G = 0$ input.

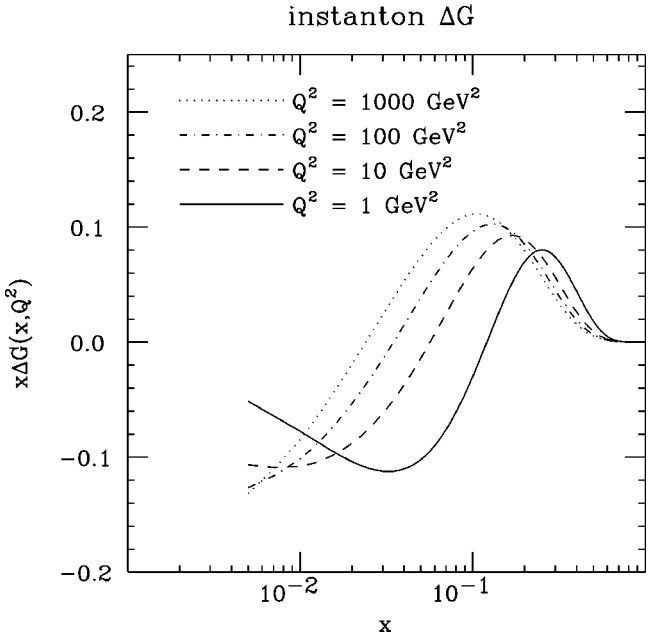


FIG. 7. Same as Fig. 5 and Fig. 6 for the instanton gluon input.

There are a number of basic physical assumptions underlying these distributions. First, the valence distributions are SU(6) motivated and the $\Delta q_v$ parametrizations are determined using the Bjorken sum rule. The SU(3) sea symmetry is broken due to mass effects in polarizing the heavier strange quarks. Then, we generate $\Delta q$ from $q$ under well defined phenomenological assumptions. Our choice of $\eta(x)$ yields a small-$x$ behavior which is Regge-like and a large $x$ behavior satisfying the counting rules. We have assumed no unphysical large $\Delta G$ and $L_z$, but have allowed an explicit interplay between $\Delta S$ and $\Delta G$ via the anomaly in the CI factorization. The three different polarized gluon models have different physical bases and provide a reasonable range

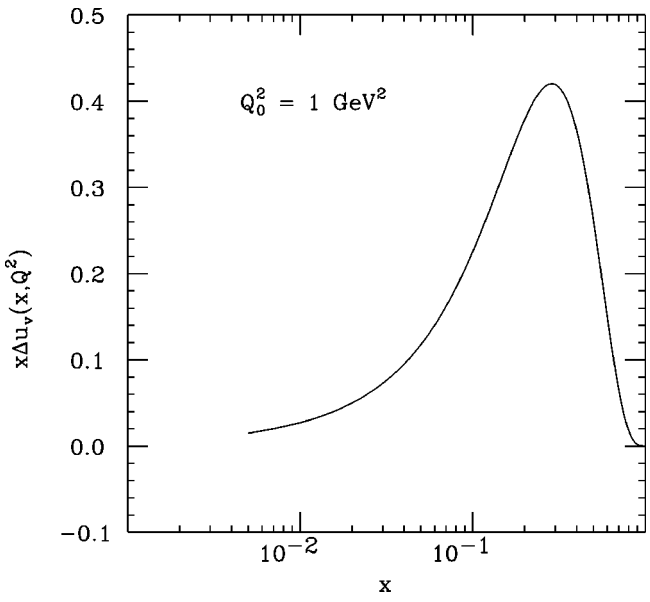


FIG. 8. Polarized valence up quark ($u_v$) distribution at low $Q^2$ for the different gluon models.

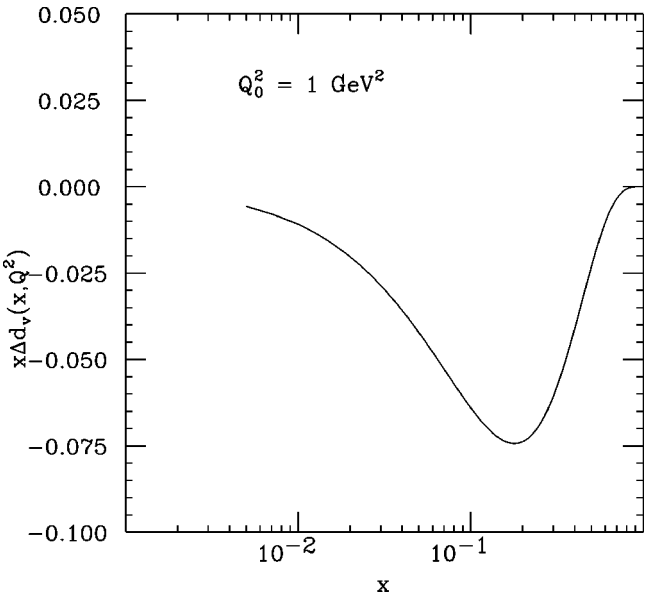


FIG. 9. Polarized valence down quark ($d_v$) distribution at low $Q^2$ for the different gluon models.

of possibilities, which can be narrowed down by future experiments. These gluon models are consistent with theoretical calculations involving quark models and assumptions about the orbital angular momentum [16,35,36].

The distributions exhibit success in fitting $g_1^{p,n,d}$ both in $x$ dependence and the integral values: $\int_0^1 g_1^{p,n,d} dx$, since these are built into the parametrizations. Evolution has been performed in LO and NLO, with little significant difference in the range $1\ \mathrm{GeV}^2 \leqslant Q^2 \leqslant 10\ \mathrm{GeV}^2$. Differences start becoming apparent at the $Q^2$ values of other experiments (around $40-50\ \mathrm{GeV}^2$). This will be discussed in more detail in [29].

In Sec. III, we discussed the allowable range of $n$ and $b$ in $\eta(x)$, subject to the positivity constraint, with $a$ fixed by normalization to data. These two parameters are tightly constrained together. Thus any variation in $n$, will restrict the

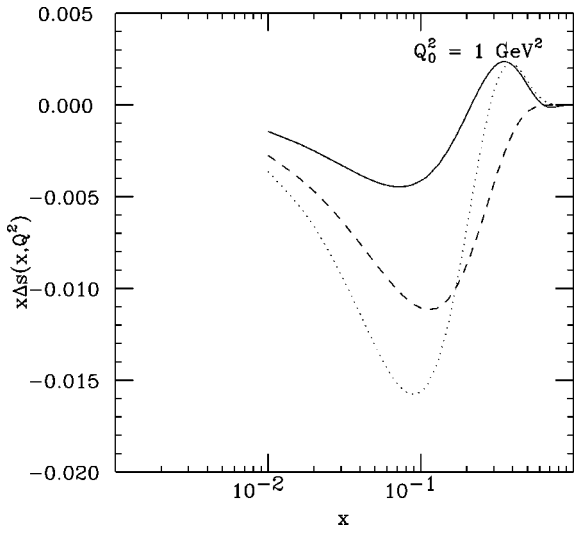


FIG. 10. Polarized up and down sea ($\bar{u}+\bar{d}$) distribution at low $Q^2$ for the different gluon models.

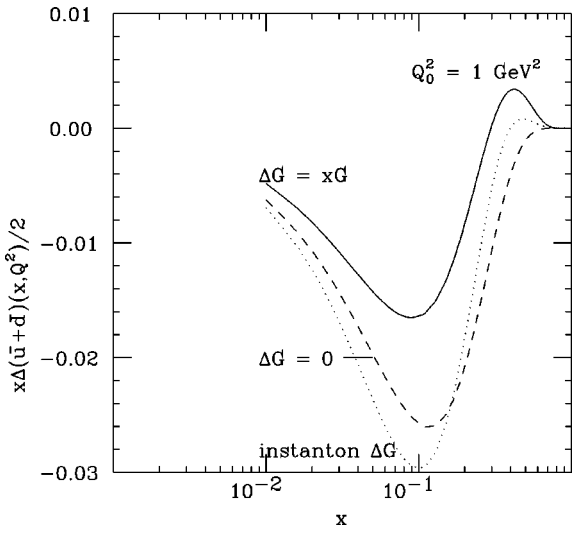


FIG. 11. Polarized strange sea ($\bar{s}$) distribution at low $Q^2$ for the different gluon models.

allowable values of $b$, with the most flexibility for about $\frac{1}{2} \leqslant n \leqslant 1$. The corresponding possible variation in $b$ is comparable to the range of $a$ seen in Tables I through III for fixed values of $b$. The variation in $a$ is primarily due to the different $\eta_{av}$ values, characteristic of the different experimental results. This range is not significantly large, and since the polarized sea is only a small part of $g_1$, except perhaps at small-$x$, the differences are not significant to the overall results we present here.

The results of $g_1^p$ at small-$x$ imply that it may be possible to narrow down the gluon size with more precise PDIS experiments at small-$x$. Such experiments are planned at SLAC (E155) and DESY (HERMES). These would also refine the parametrizations by indicating the behavior of $g_1^i$ at small-$x$. Comparisons of the $x$-dependent deuteron structure function with the corresponding proton and neutron structure functions could provide insight into possible nuclear effects, if they are significant. There are various possible experiments which would provide a better indication of the size of the polarized gluon distribution. These include (1) one and two jet production in $e-p$ and $p-p$ collisions [45,46,47,48], (2) prompt photon production [18,49,50,51,52], (3) charm production [53] and (4) pion production [47]. Groups at the BNL Relativistic Heavy Ion Collider (RHIC) (STAR), SLAC (E156), CERN (COMPASS) and DESY (HERA-$\vec{N}$) are planning to perform these experiments in the near future. For detailed explanations of these experiments, see [54]. We are presently calculating the appropriate processes using the distributions and gluon models presented here [29].

## ACKNOWLEDGMENTS

One of us (G.P.R.) would like to thank P. Ratcliffe and D. Sivers for useful discussions regarding the positivity constraint. This work was supported in part by the U.S. Department of Energy, Division of High Energy Physics, Contract W-31-109-ENG-38.

[1] M. Goshtasbpour and G. P. Ramsey, Phys. Rev. D **55**, 1244 (1997).
[2] J. Ellis and M. Karliner, Phys. Lett. B **341**, 397 (1995).
[3] T. P. Cheng and L.-F. Li, Phys. Rev. Lett. **74**, 2872 (1995); Phys. Rev. D **57**, 344 (1998).
[4] R. D. Ball, S. Forte, and G. Rudolfi, Nucl. Phys. **B444**, 287 (1995); **B449**, 680E (1995); **B496**, 337 (1997); R. Ball *et al.*, hep-ph/9707276; G. Altarelli, R. D. Ball, S. Forte, and G. Rudolfi, Acta Phys. Pol. B **29**, 1145 (1998).
[5] T. Gehrmann and W. J. Stirling, Z. Phys. C **65**, 461 (1995).
[6] M. Glück, E. Reya, M. Stratmann, and W. Vogelsang, Phys. Rev. D **53**, 4775 (1996).
[7] J. Bartelski and S. Tatur, Z. Phys. C **71**, 595 (1996).
[8] D. DeFlorian, O. A. Sampayo and R. Sassot, Phys. Rev. D **57**, 5803 (1998).
[9] D. Indumathi, Z. Phys. C **64**, 439 (1994).
[10] K. Abe *et al.*, Phys. Rev. Lett. **78**, 815 (1997); Phys. Rev. D **54**, 6620 (1996); Phys. Rev. Lett. **74**, 346 (1995); Phys. Lett. B **364**, 61 (1995); P. L. Anthony *et al.*, Phys. Rev. Lett. **71**, 959 (1993).
[11] K. Abe *et al.*, Phys. Rev. Lett. **79**, 26 (1997).
[12] P. L. Anthony *et al.*, Phys. Rev. D **54**, 6620 (1996).
[13] K. Ackerstaff *et al.*, Phys. Lett. B **404**, 383 (1997).
[14] B. Adeva, *et al.*, Phys. Lett. B **320**, 400 (1994); D. Adams *et al.*, *ibid.* **329**, 399 (1994); **357**, 248 (1995); Phys. Rev. D **56**, 5330 (1997).
[15] B. Adeva *et al.*, Phys. Lett. B **369**, 93 (1996).
[16] S. J. Brodsky, M. Burkardt, and I. Schmidt, Nucl. Phys. **B441**, 197 (1995).
[17] R. Carlitz and J. Kaur, Phys. Rev. Lett. **38**, 673 (1977); J. Kaur, Nucl. Phys. **B128**, 219 (1977); F. E. Close, H. Osborn, and A. M. Thomson, *ibid.* **B77**, 281 (1974).
[18] J.-W. Qiu, G. P. Ramsey, D. G. Richards, and D. Sivers, Phys. Rev. D **41**, 65 (1990).
[19] S. A. Larin, F. V. Tkachev, and J. A. M. Vermaseren, Phys. Rev. Lett. **66**, 862 (1991); S. A. Larin and J. A. M. Vermaseren, Phys. Lett. B **259**, 345 (1991); A. L. Kataev and V. Starshenko, Mod. Phys. Lett. A **10**, 235 (1995).
[20] A. D. Martin, R. G. Roberts, and W. J. Stirling, Phys. Lett. B **387**, 419 (1996).
[21] H. L. Lai *et al.*, Phys. Rev. D **55**, 1280 (1997); **51**, 4763 (1996); W.-K. Tung, hep-ph/9608293.
[22] F. Close and D. Sivers, Phys. Rev. Lett. **39**, 1116 (1977).
[23] P. Chiapetta and J. Soffer, Phys. Rev. D **31**, 1019 (1985).
[24] E. Stein *et al.*, Phys. Lett. B **353**, 107 (1995).
[25] G. Rossi, Phys. Rev. D **29**, 852 (1984).
[26] W. Vogelsang, Nucl. Phys. **B475**, 47 (1996); Phys. Rev. D **54**, 2023 (1996).
[27] M. Hirai, S. Kumano, and M. Mayama, Comput. Phys. Commun. **108**, 38 (1998).
[28] A. J. Buras, Rev. Mod. Phys. **52**, 199 (1980); E. Reya, Phys. Rep. **69**, 195 (1981).
[29] L. E. Gordon and G. P. Ramsey, ANL-HEP-PR-98-92.
[30] G. Bodwin and J.-W. Qiu, Phys. Rev. D **41**, 2755 (1990).
[31] Adler and W. Bardeen, Phys. Rev. **182**, 1517 (1969).
[32] For a detailed discussion and comparison of these schemes, see H.-Y. Cheng, Int. J. Mod. Phys. A **11**, 5109 (1996); Phys. Lett. B **427**, 371 (1998).
[33] A. V. Efremov and O. V. Teryaev, JINR Report E2-88-287 (1988); G. Altarelli and G. G. Ross, Phys. Lett. B **212**, 391 (1988); R. D. Carlitz, J. C. Collins, and A. H. Mueller, *ibid.* **214**, 229 (1988).
[34] D. L. Adams *et al.*, Phys. Lett. B **336**, 269 (1994); D. P. Grosnick *et al.*, Phys. Rev. D **55**, 1159 (1997).
[35] V. Barone, T. Calarco, and A. Drago, hep-ph/9801281.
[36] I. Balitsky and X. Ji, Phys. Rev. Lett. **79**, 1225 (1997).
[37] J. Blümlein and N. Kochelev, *Deep Inelastic Scattering and QCD, 5th International Workshop*, AIP Conf. Proc. No. **407** (AIP, New York, 1997), p. 875; DIS97, Chicago, IL, edited by J. Repond and D. Krakauer.
[38] F. Antonuccio, S. J. Brodsky, and S. Dalley, Phys. Lett. B **412**, 104 (1997).
[39] F. Close and R. G. Roberts, Phys. Lett. B **336**, 257 (1994).
[40] A. Donnachie and P. V. Landshoff, Z. Phys. C **61**, 139 (1994).
[41] S. D. Bass and P. V. Landshoff, Phys. Lett. B **336**, 537 (1994).
[42] A. H. Mueller and T. L. Trueman, Phys. Rev. **160**, 1306 (1967); L. Galfi, J. Kuti, and A. Pathos, Phys. Lett. B **31**, 465 (1970); F. E. Close and R. G. Roberts, Phys. Rev. Lett. **60**, 1471 (1988).
[43] R. L. Heimann, Nucl. Phys. **B64**, 429 (1973).
[44] J. Ellis and M. Karliner, Phys. Lett. B **213**, 73 (1988).
[45] M. Stratmann and W. Vogelsang, Z. Phys. C **74**, 641 (1997).
[46] G. P. Ramsey, D. Richards, and D. Sivers, Phys. Rev. D **37**, 3140 (1988).
[47] G. P. Ramsey and D. Sivers, Phys. Rev. D **43**, 2861 (1991).
[48] L. E. Gordon, Phys. Rev. D **57**, 235 (1998).
[49] L. E. Gordon and W. Vogelsang, Phys. Lett. B **387**, 629 (1996).
[50] L. E. Gordon and W. Vogelsang, Phys. Rev. D **49**, 170 (1994).
[51] A. P. Contogouris and Z. Merebashvili, Phys. Rev. D **55**, 2718 (1997).
[52] C. Coriano and L. E. Gordon, Phys. Rev. D **49**, 170 (1994); **54**, 781 (1996).
[53] B. Baily, E. L. Berger, and L. E. Gordon, Phys. Rev. D **54**, 1896 (1996).
[54] G. P. Ramsey, Prog. Part. Nucl. Phys. **39**, 599 (1997); Part. World **4**, 11 (1995).